AIMS Energy, 8(5): 835–858.
DOI: 10.3934/energy.2020.5.835
Received: 17 June 2020
Accepted: 27 August 2020
Published: 03 September 2020

http://www.aimspress.com/journal/energy

Research article

Comparative study between the simulation and experimental results of H_2 production from water vapour plasmolysis

Mostafa El-Shafie[1,*], Shinji Kambara[1], Yukio Hayakawa[1], Fahad Rehman[2]

[1] Gifu University, Environmental and Renewable Energy Systems Division, Graduate School of Engineering, 1-1 Yanagido, Gifu, 501-1193, Japan
[2] Biorefinery Engineering and Microfluidics (BEAM) Research Group, Department of Chemical Engineering, COMSATS University Islamabad, Lahore Campus, Pakistan

* **Correspondence:** Email: mostafaelshafie81@gmail.com.

Abstract: In the present study, the kinetics of hydrogen production from water vapour using dielectric barrier discharge (DBD) plasma in a cylindrical reactor were analyzed. The simulation analysis was carried out for both models with and without the dissociative attachment reaction to predict and compare the concentration of produced hydrogen gas from water vapour. The effect of water vapour input temperature ranges of 523–623 K and plasma voltage in the range of 12–14 kV were investigated. It was revealed that the hydrogen concentration increased with the input water vapour temperature and plasma voltage increased in both the simulation models. It was seen that the H_2 concentration results of the simulation model with the dissociative attachment reaction (H^-) were nearly same as the H_2 concentrations of the water vapour plasmolysis experimental results. Moreover, it can be concluded that the dissociative attachment reaction was controlled the H_2 generation from water vapour plasmolysis. It was remarkable that the conversion rates of the simulation model included the dissociative attachment reaction has more acceptable results to the experimental data compared to the simulation model deselecting the dissociative attachment reaction (H^-). Also, it was seen as the main reason for the difference between simulation and experimental results.

Keywords: hydrogen production; DBD plasma; water vapour; conversion rate

1. Introduction

Many substantial research efforts have been carried out to use hydrogen as an alternative energy carrier [1]. It is agreed with all environmental issues related to the usage of the conventional fuels such as exhaustion, pollution and climate change [2]. One of the great challenge faced the hydrogen production process is the combination between the energy sustainability and environmental protection. Different hydrogen economic studies have been investigated; it was found that the hydrogen economy offers two main advantages in terms of low greenhouse gases (GHGs) and used as an alternative fuel to reduce the consumption rate of fossil fuels [3–8]. Different hydrogen production technologies have been investigated [9,10]. Most of the available world hydrogen is produced by steam methane reforming process. It acts around 80–85% of the total world hydrogen and the remaining is produced by water electrolysis and coal gasification methods [11]. Currently, methane is obviously considered the best choice of fossil fuels due to its availability and low GHGs emissions [12]. Also, hydrogen can be produced by the water electrolysis process which is considered a commercial method [13]. In addition, Hydrogen gas has been generated by thermochemical methods from the biomass process as a renewable and sustainable energy source [14]. Most of the hydrogen production technologies are directly or indirectly utilized fossil fuels, subsequently GHGs are emitted.

Water vapor plasmolysis is mostly considered as a clean hydrogen energy carrier which the hydrogen can be generated without any environmental impact. Plasma is generated using the electrical energy which transformed into electron kinetic energy then water molecules excitation and produce hydrogen and oxygen gas [15,16]. The high productivity and efficiency is behind the continuous interest in hydrogen production using the non-thermal plasma or dielectric barrier discharge plasma (DBD plasma). Hydrogen production from water vapor using plasma has been viewed as a high expensive method, additionally; the efficiency has been registered value of 50% compared with the conventional plasma reactors [15,17]. Plasmolysis has the ability to produce hydrogen 1000 times more than the water electrolysis process due to the multiple excited species are produced by applying plasma, in addition, it was reported that the energy efficiency of the plasma chemical reaction is same as thermos-catalytic and electrolytic methods [18].

Different feed stocks have been utilized in plasma-chemical processes such as methanol, ethanol, kerosene, and water in liquid and vapor state [19–27]. The kinetic models of the hydrogen production from water vapor using DBD plasma have been developed [28]. The hypothesis of this study is to simulate the hydrogen production from water vapor plasmolysis over a period of time that will lead to predict the chemical kinetics and compared it with the H_2 concentration of the experimental results under the same operating conditions. Two water vapor plasmolysis kinetic models are simulated for a cylindrical type reactor. The simulation analysis was carried out using non-thermal plasma at atmospheric pressure and incorporated with the initial species concentration. The effects of the dissociative attachment reaction on the simulation results of water vapor break down into hydrogen and oxygen gas were evaluated. The species concentrations at steady state were monitored for both simulation models. The hydrogen concentrations results were compared for both tested models and the H_2 concentration of experimental results. Also, the H_2 conversion rates of both models and experimental results were analyzed.

1.1. Methods of simulation analysis

In this study, the concentrations of product gases of water vapor plasmolysis were simulated and investigated in a cylindrical type DBD plasma reactor using Reaction Engineering Lab of COMSOL Multphysics ^{TM}. A few reactions are presented to describe the hydrogen formation from water vapour plasmolysis because we used the water vapour plasmolysis reaction kinetic model suggested by Fahad et al. [28]. The complete reaction mechanism is shown in Table (1). The simulation analysis was carried out for the water vapor decomposition with several mechanisms including dissociative ion attachment and dissociation reaction but without ionization reaction. Also, the simulation is implemented by excluding the dissociative attachment reaction (H^-). The first model was excluded (reaction no (2)) in Table (1) to evaluate the effect of the dissociative attachment reaction (H^-) on the water vapor dissociation reaction mechanism pathway, while the second one used the full reaction mechanism in Table (1) including the dissociation reaction and the dissociative attachment reaction. However, it was reported that the dissociative attachment reaction (reaction (2)) was an important step for water vapor breakdown using plasma [28].

The experimental species concentrations data are utilized as input data to the simulation models to investigate the water vapour decomposition reaction mechanism pathway. The experimental and simulation results are deeply investigated and compared in section 3. In this reaction mechanism, water vapor is decomposed to generate hydrogen and oxygen molecules after a chain of reactions. The kinetics of H_2 formation from water vapor decomposition in a cylindrical type reactor was studied by applying DBD plasma. The water vapor density was determined at the water vapor temperature ranges of 250–350 ℃ using the ideal gas law. This simulation study results were compared with the experimental water vapor decomposition data and the pathway of reactions consists of six chemical reactions.

Table 1. Simulated reaction mechanism.

No.	Reaction type	Type	Rate constant (K) [m^3/mol-sec, m^6/mol-sec]	Ref.
1	$H_2O + e \rightarrow H + OH + e$	Dissociation reaction	9.978E+07	[29,30]
2	$H_2O + e \rightarrow H^- + OH$	Dissociative attachment	3.706E+07	[13,29]
3	$OH + OH \rightarrow H_2O_2$	Neutral-neutral reaction	1.02E+07	[30]
4	$OH + H_2O_2 \rightarrow H_2O + HO_2$	Neutral-neutral reaction	1.02E+06	[30]
5	$HO_2 + HO_2 \rightarrow H_2O_2 + O_2$	Surface reaction 1	9.64E+05	[30]
6	$HO_2 + H \rightarrow H_2 + O_2$	Surface reaction 2	3.91E+07	[30]

Many studies have been carried out to model the water vapor decomposition using DBD plasma. The overall water vapor kinetic models and single type plasmo-chemical reactions like ionic collision for the water vapor have been investigated in different studies [15,18,31,32]. A zero dimensional model has been proposed for low density non-stationary discharge gas in water vapor by Avtaeva et al. [31]. The water vapor at very low pressure (133–150 kPa) have been studied, the results showed that the most positive and negative species were H_3O^+ and OH^-, respectively [31]. The effect of dissociative attachment reaction number (2) in table (1) included negative hydrogen a radical (H^-) on the hydrogen production in cylindrical reactor was observed on the hydrogen formation kinetics. In the current study, two reaction mechanisms of water vapor dissociation are

simulated for hydrogen production with and without the dissociative attachment reaction (H^-). The simulation results are compared with the experimental hydrogen concentrations results.

The water vapor plasmolysis dissociation direct decomposition pathway can be expressed as follows [13]:

$$H_2O \rightarrow H_2 + \frac{1}{2}O_2 \qquad \Delta H = 2.6\ \text{eV/mol} \tag{1}$$

The primary species of water vapor decomposition are hydrogen and hydroxyl radicals [33]. The dissociation reaction of produced atomic hydrogen and hydroxyl radicals can be written as follows [33–35]:

$$H_2O + e \rightarrow H + OH + e \tag{2}$$

The water vapor decomposition using DBD plasma is formed most of reactive species such as hydroxyl OH, H atoms, and oxygen atoms O^-. It was associated that the primary chemical reaction produced species H and OH radicals, then these species react with each other to generate molecular products such as hydroperoxyl HO_2 [36]. The chemical reactions pathway included the negative species (OH^-, H^-, and O^-) of water vapor have also been reported [31,32]. Also, it was reported that the following reactions may happen in the water vapor plasmolysis but it has low probability and required a relative high energy [32], therefore, these reactions are not included in the current simulation studies.

$$H_2O + e \rightarrow O^+ + 2H + 2e \tag{3}$$

$$H_2O + e \rightarrow H^+ + O + H + 2e \tag{4}$$

$$H_2O + e \rightarrow 2H + O + e \tag{5}$$

The simulation reaction mechanism of water vapor plasmolysis by the dissociative attachment of electrons was included and water vapor dissociation is initiated with the dissociative attachment of an electron (H^-). In this simulation study, the effect of dissociative attachment reaction (H^-) was investigated on the water vapor decomposition using DBD plasma. The negative hydrogen radical (H^-) formed in the full reaction mechanism combines with the electron through electron detachment process as follows:

$$H^- + e \rightarrow H + e + e \tag{6}$$

In the current simulation study, the reaction mechanism model was proposed and analyzed for both different mechanism pathways of the water vapor dissociation. The reaction kinetic models were implemented using Reaction Engineering Lab. (REL) in COMSOL Multiphysics^{TM} [37]. This package provides an automatic sensing of stiff systems and an adaptive time stepping algorithm with tolerance of 10^{-6} [38].

1.2. Initial boundary conditions

The initial concentration of water vapor was determined using the ideal gas law at the given water vapor temperature and atmospheric pressure. In this simulation study, water vapor and electrons are the only input reactants to the system. The initial number of electron density was set

at 10^6 m^{-3} due to cosmic radiation. Furthermore, it was found that the equilibrium electron density values for non-thermal (DBD) plasma vary in a range of (10^{18}–10^{21} m^{-3}) [39,40]. While it was experimentally reported that the lowest value of electron density was 10^{17} m^{-3} [41]. However, the general electron density whole range of (10^{18}–10^{21} m^{-3}) was applied for both models to investigate the water vapour plasmolysis kinetic behavior. The input plasma voltage ranges of 12–14 kV and pure water vapor flow rate of 0.0104 L/min were used at different water vapor temperatures range of 523–623 K. The hydrogen and oxygen gas species experimental concentrations data were set as input data.

2. Experimental description and conditions

In this study, pure water vapor was decomposed using DBD plasma in a cylindrical type reactor. The DBD plasma was generated between quartz glass and stainless steel surfaces at atmospheric pressure, while the discharge gap between surfaces was 1 mm. The water vapor plasmolysis experiment was carried out at a constant feeding flow rate of 0.0104 L/min, plasma applied voltage of 12–14 kV and temperature ranges of 250–350 ℃. The outlet gas samples are taken after gas separated in the ice trap by using syringe then the hydrogen, oxygen, and nitrogen concentrations are measured by gas chromatography (GC). The plasma reactor volume was 5.296 cm^3. The hydrogen concentration was measured using gas chromatography (GC) model type of GC-2014S, SHIMADZU, in addition, the water vapor decomposition experiments were repeated two times. Furthermore, the GC error was estimated before starting the water plasmolysis experiments within ±5% by using standard gas concentrations. The water vapor was generated using the steam generator and the steam flow rate was controlled by mass flow controller while the pressure was monitored using the digital pressure gauges. Figure (1) represents the schematic diagram of the water vapor decomposition process in cylindrical type reactor. The discharge voltage was applied at frequency of 10 kHz. The decomposed gases were separated using the ice trap and the sample was collected using syringe. The current study aims to investigate the hydrogen production from water vapor using DBD plasma. The hydrogen production experiments were carried out using different range of the operational parameters as mentioned above.

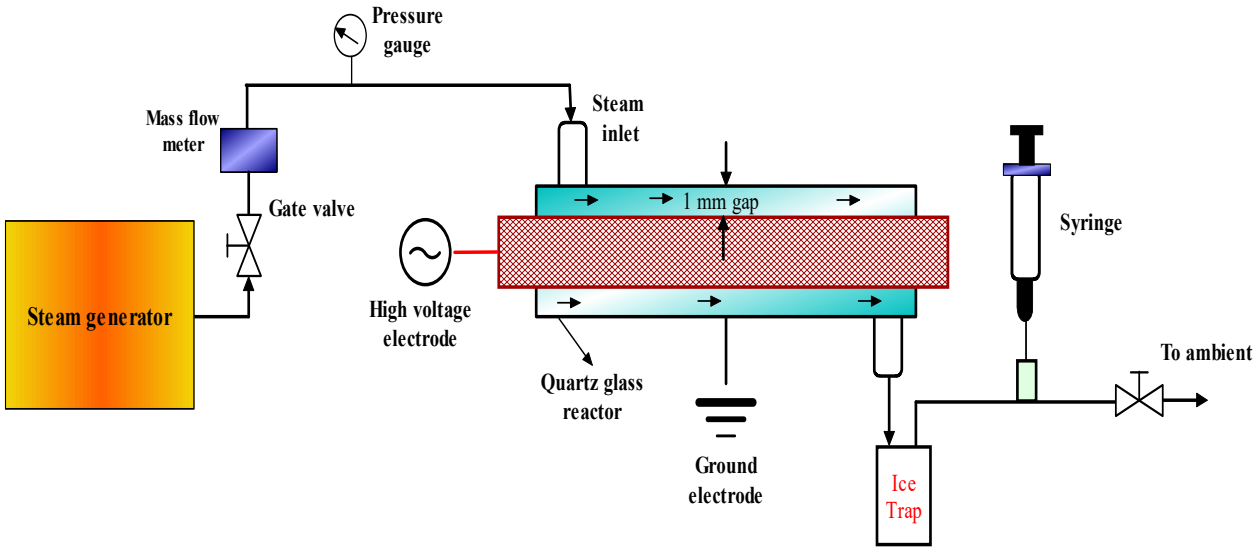

Figure 1. Schematic diagram of hydrogen production using DBD plasma in a cylindrical type reactor.

3. Results and discussion

Figure (2) shows the plasma ignition test photos at plasma voltage range of 10–18 kV. The plasma ignition lighting is enhanced with the typical applied voltage increase. The total electrical power input to the DBD plasma is not the same as the total power consumption due to the lag of the voltage phase angle compared to the current phase angle [42]. The applied frequency of DBD plasma was adjusted at 10 kHz, the typical electric plasma power for one oscillation period can be determined as follows [43]:

$$P = VI\cos\varphi \tag{8}$$

$$I = \frac{V}{Z} \tag{9}$$

$$P = \frac{1}{2}\frac{V^2}{|Z|}\cos\varphi \tag{10}$$

Where the plasma voltage amplitude is V, the plasma current is I, Z is the impedance, and φ is the phase angle between voltage amplitude and current. Therefore, it was investigated that the power consumption in the DBD plasma is lower than the total plasma power utilized in the water vapor decomposition process. In addition, the total actual power consumed (P_{total}) can be calculated using the current (I_{peak}) and voltage (V_{peak}) peak values as follow [44]:

$$P_{total} = V_{peak} \times I_{peak} \tag{11}$$

The concentration of produced hydrogen gas with time was measured at different water vapor input temperatures and plasma applied voltage ranges of 12–14 kV. It was reported that the negative species (H^-) will combine due to their weak cross sections ($1 - 6 \times 10^{-18}$ cm^2 per molecule). Furthermore, the electron energies were in a range of 6–12 eV [32].

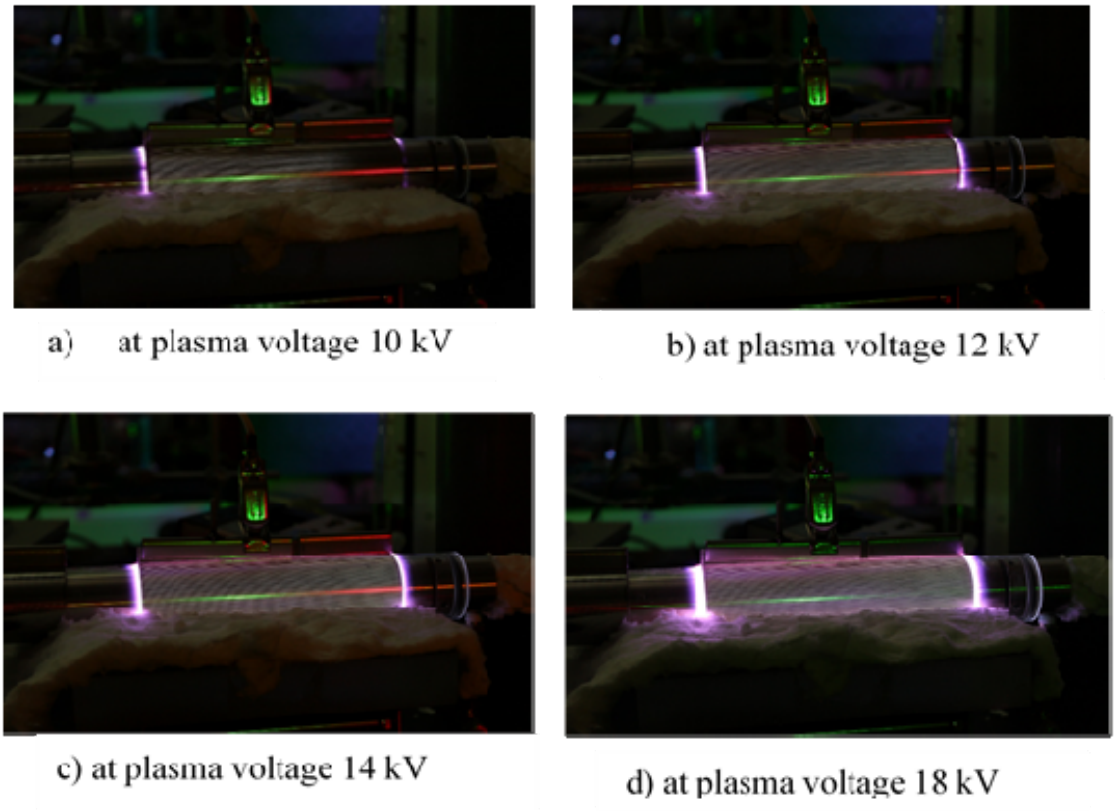

Figure 2. Steam decomposition at different plasma applied voltage.

3.1. Simulation model I (without dissociative attachment reaction)

The first simulation analysis was carried out without or by deselecting the dissociative attachment reaction. In this simulation model, the effect of dissociative attachment reaction on the concentration of hydrogen production from water vapor was analyzed by deselecting it from reaction scheme. The simulation results were used the experimental results data and the simulation analysis was carried out at the same operating conditions. The steady state concentration of the water vapor decomposition species without dissociative attachment reaction was introduced in Figure (3). The input species concentrations data of this figure were taken from the experimental data, the experimental outlet hydrogen and oxygen concentrations were measured by GC were also used as a simulation input data. Atypical 99% of the concentrations of water vapor plasmolysis species are found such as H_2, O_2, OH, etc. at time scale 0.01s [28,45]. In the absence of the dissociative attachment reactions, water vapour concentration is reach to the steady state and more H atoms are generated with the increasing of the electron concentration. Moreover, the recombination of hydrogen atoms is the main source of hydrogen gas. The simulation result of steady state hydrogen gas concentration versus the evolution time is shown in Figure (4). It was clear that the hydrogen concentration increases with the reaction time scale until reach to the steady state. It was found that the hydrogen concentration increased continuously with the reaction time scale. Also, it was reported that the reaction of water vapor plasmolysis should be completed before the ions or gas particles reach to the reactor wall or to the electrode surfaces [38]. Also, different water vapor plasmolysis models have been simulated and the species spectra showed (H, OH, O, etc.,) have been obtained [31,45,46].

Figure (5) illustrates the water vapour concentration simulation results without the dissociative attachment reaction (H^-) over the time. It was clear from the simulation result that the total input water vapours are decomposed into their elements and the concentration of water vapour reach to zero. Although, some of the outlet hydrogen and oxygen gases are recombined in the ice trap by means experimental results showed a condensed water vapor inside the ice trap. Furthermore, this model results did not seem to be accurate because of the water vapour did not completely convert into hydrogen and oxygen in the real experiment. The outlet species concentrations of the experimental results at water vapor temperature of 523 K and plasma voltage of 12 kV are shown in Figure (6). The results of the analyzed gas samples showed the concentration of the following species of (H_2, O_2, and N_2), in addition some of hydrogen and oxygen gas are recombined to compose water inside the ice trap.

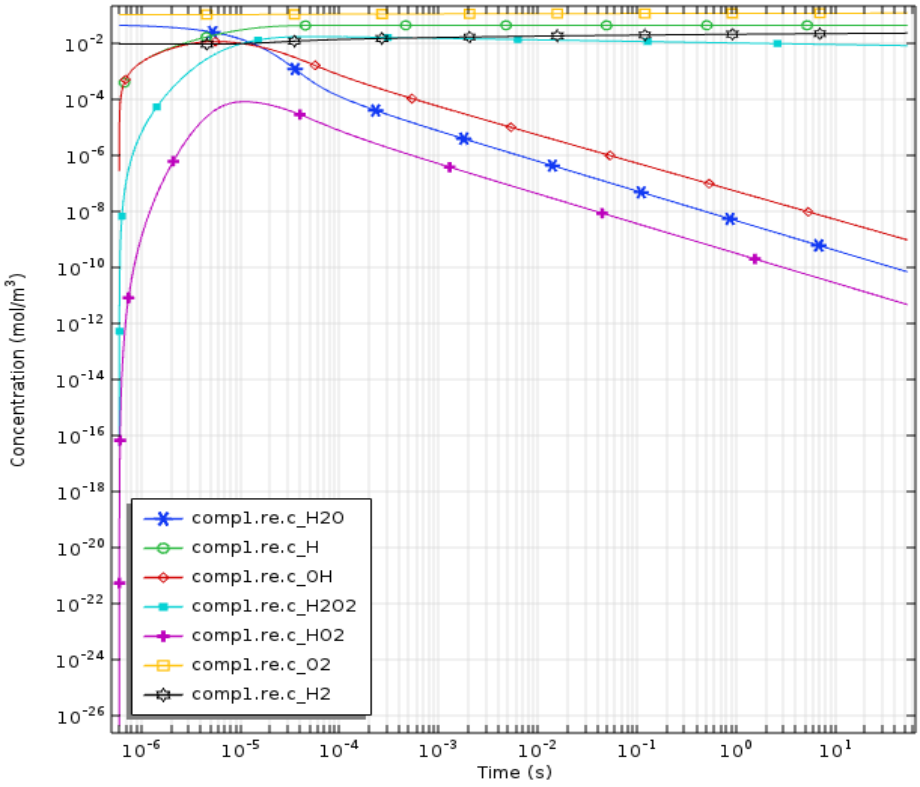

Figure 3. Concentration profiles of the outlet species versus the evolution time (Model I).

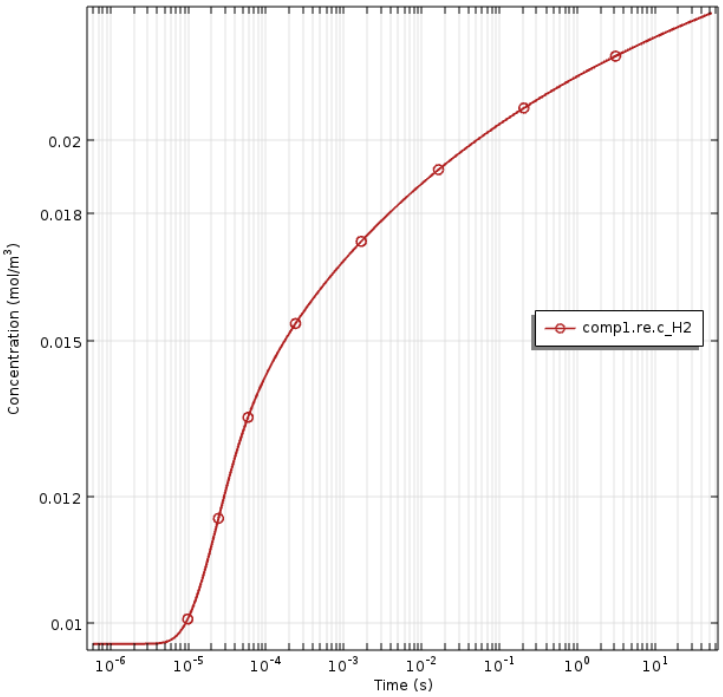

Figure 4. H_2 profile concentration versus evolution time (Model I).

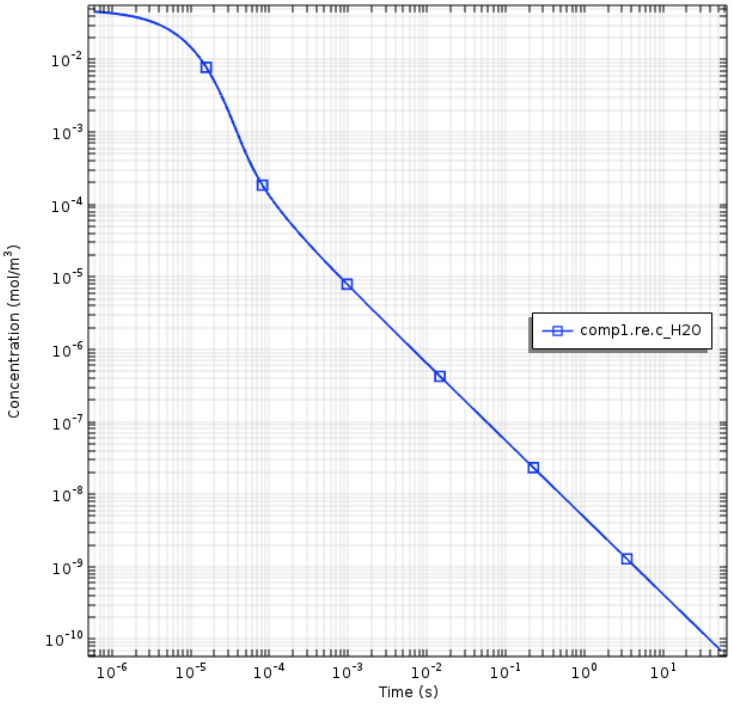

Figure 5. H_2O profile concentrations versus evolution time (Model I).

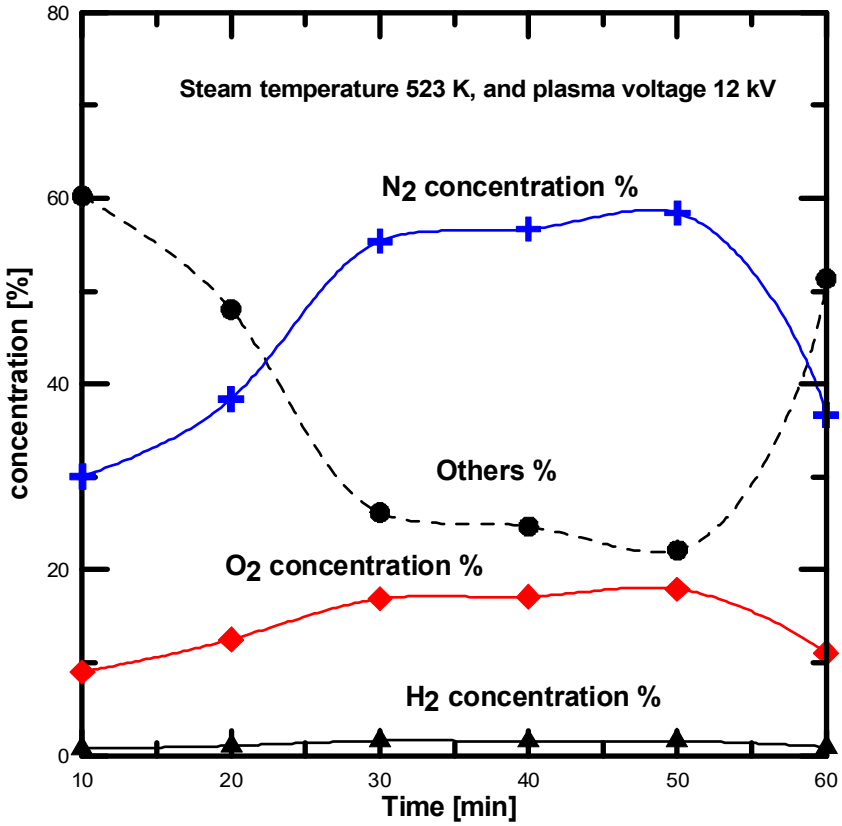

Figure 6. Experimental results of outlet species concentrations of water vapor decomposition.

It was observed that the nitrogen gas concentration is included in the outlet species because of there are some of air content in the water vapour pathway line, also, it is possible that some of air was entered to syringe during the sample collections [45]. Furthermore, the hydrogen, oxygen, and nitrogen gas concentrations are typically showed the same profile trend, also, it can be concluded that the hydrogen concentration result of water vapour plasmolysis is not affected by air leakage because of the leakage air is not involved in the activated plasma reaction area. Additionally, it was found that the concentrations trend of H_2, O_2, and N_2 decreased at the end of the dissociation time due to more of produced H_2 and O_2 gas are recombined again to compose water molecules which resulted in the increasing of the concentration of the trend of others. To clarify the effect of water vapor decomposition deselecting the dissociative attachment reaction on the simulation results, a comparison between simulation and experimental results will discuss in the next section.

3.1.1. Comparison between theoretical and experimental results (Model I)

The simulation model of water vapor plasmolysis without dissociative attachment reaction (H^-) (reaction (2)) was analyzed and compared with the water vapor decomposition experimental data. Figure (7) shows the effect of inlet water vapor temperature on the hydrogen production concentration over time at plasma applied voltage of 12 kV. The simulation results are obtained at different operating temperatures, it was found that the hydrogen concentration increased with the inlet water vapor temperature at the same plasma applied voltage [16].

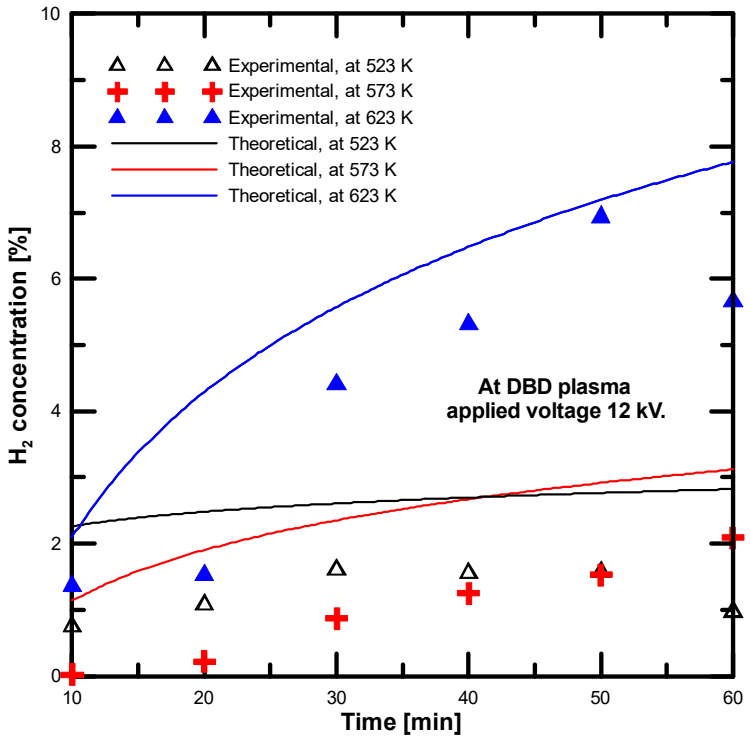

Figure 7. Comparison between experimental and theoretical steam decomposition concentrations data at plasma voltage 12 kV.

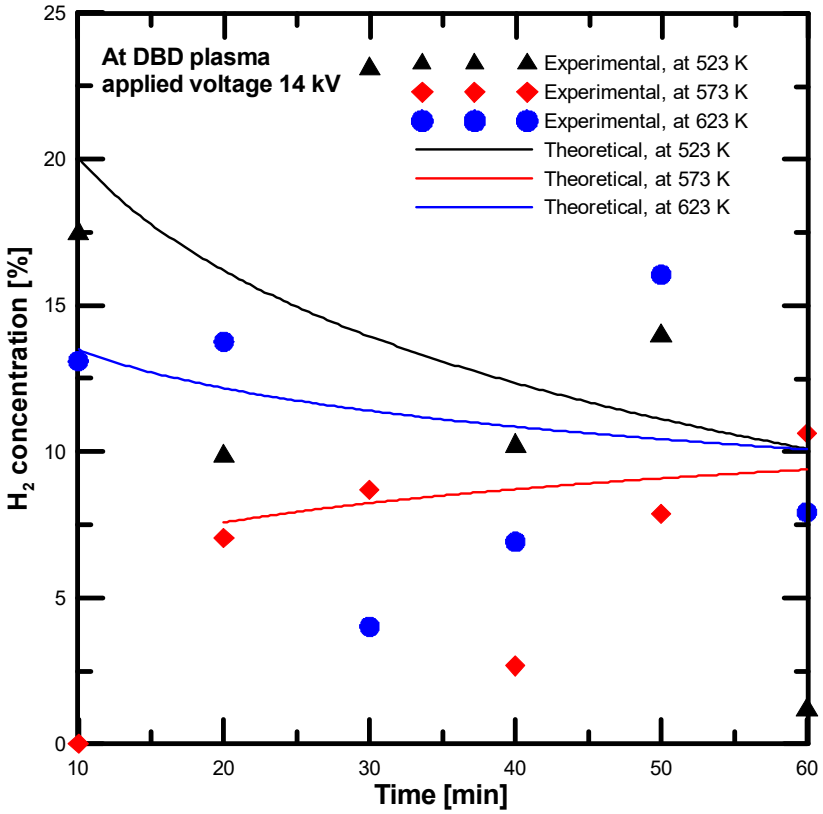

Figure 8. Comparison between experimental and theoretical steam decomposition concentrations data at plasma voltage 14 kV.

Furthermore, the hydrogen concentration of the simulation results without the dissociative attachment reaction was always showed that the H_2 concentration was higher than that obtained from the experimental results because of model I did not include the H^- radicals. As discussed before, the main reason of the decreasing of hydrogen concentration at the end of the dissociation time due to the recombination of H_2 and O_2 gas inside the ice trap, also, it was reported that some of the separated H_2 gas are still remained inside the ice trap.

Figure (8) describes the effect of inlet water vapor temperature at plasma applied voltage of 14 kV with time. It was found that the hydrogen concentration decreased with time but the hydrogen concentration values are higher than that obtained from plasma voltage 12 kV. The simulation and experimental results of H_2 concentration for low water vapor temperature of 523 K were higher than that obtained from high water vapor temperature due to the syringe sample collection error and the measurement procedures; it is possibly changed due to the change of the measurements accuracy and the separation procedure of the product gases.

The effect of plasma applied voltage on the hydrogen production from water vapor decomposition using DBD plasma and at constant temperature in ranges of 523–623 K are shown in Figure (9a, b, c). It was found that the hydrogen concentration results of applied voltage 14 kV were higher than 12 kV at the same input temperature. Furthermore, this figure indicates that the simulation of H_2 concentration results at plasma voltage of 12 kV were higher than experimental results, while the concentration results at plasma voltage of 14 kV decreased with time scale and also are not same as the simulation results. The simulation results of hydrogen concentration at plasma applied voltage 12 kV were higher than experimental, these results were confirmed the results of deselecting the dissociative attachment (reaction no. (2) in Table (1)) that investigated by Fahad et al. [28]. The dissociative attachment reaction was found that has an important effect on the simulation results of the water vapor dissociation using DBD plasma and the concentration of hydrogen gas is higher than experimental values. From the analysis of simulation and experimental results, it was observed that the H_2 concentration results of the simulation model without the dissociative attachment reaction are higher than that obtained from the experimental results, also, the simulation trend profiles are changed according to the H_2 concentrations obtained from the water vapour dissociation experiments.

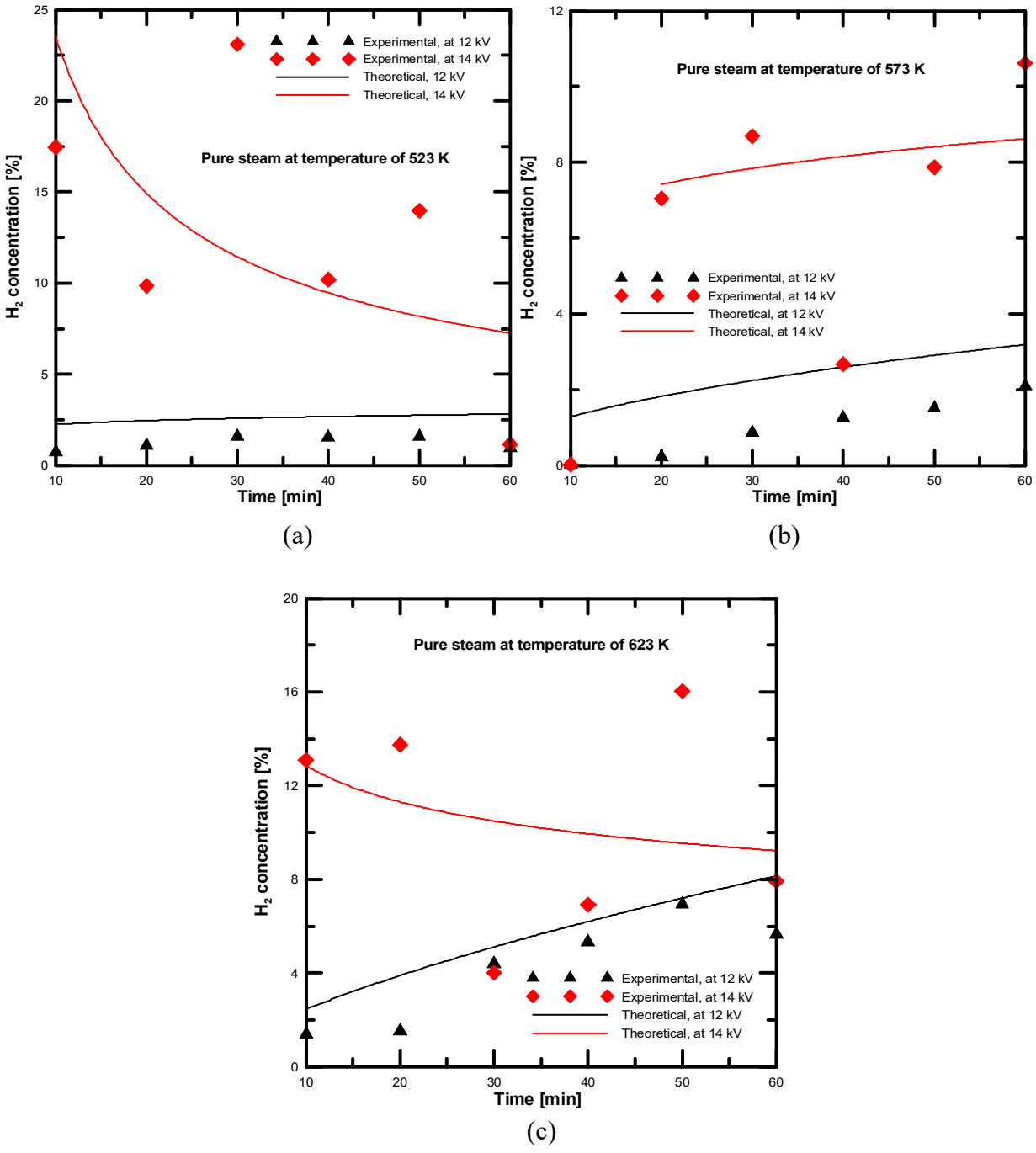

Figure 9. Comparison between experimental and theoretical results of H_2 concentration at different input water vapor temperatures.

3.2. Theoretical analysis of water vapor decomposition using DBD plasma with dissociative attachment reaction

In this simulation model, the full reaction mechanism included the dissociative attachment reaction (H^-) was analyzed. The dissociative attachment reaction included H^- was utilized to break water vapor molecules by electron impact as a first step of chains of reactions. It could be stated that the hydrogen concentration value dropped by selecting the dissociative attachment reaction [28]. Additionally, it was reported that the dissociative ionization and dissociative excitation reactions

have no effect on the kinetics as well as the species concentrations. Figure (10) shows the steady state concentration of the given full reaction mechanism species of H_2O, H, OH, H^-, H_2O_2, HO_2, O_2 and H_2 when the dissociative attachment reaction (H^-) was used. While e is expressed about the plasma discharge voltage at a frequency of 10 kHz. The concentration results of the species kinetic curves are based on a real water vapor decomposition case used in the simulation of water vapor decomposition without dissociative attachment reaction. Figure (11) indicates that the hydrogen concentration decreased from 0.025 to 0.01 moles/ m^3, it was found that the dissociative attachment reaction is an important step in the water vapor dissociation processes. Furthermore, the effect of dissociative attachment reaction (H^-) on hydrogen production from water vapor decomposition using DBD plasma was same as the simulation results obtained by Fahad et al. [28]. In addition, the simulation results of steady state water vapor concentration did not reach to zero as shown in Figure (12). It was clear that some of water vapor are not converted into hydrogen and oxygen gas, these simulation result seems to be same as the real water vapor decomposition because of some of the water vapor was remained in the ice trap.

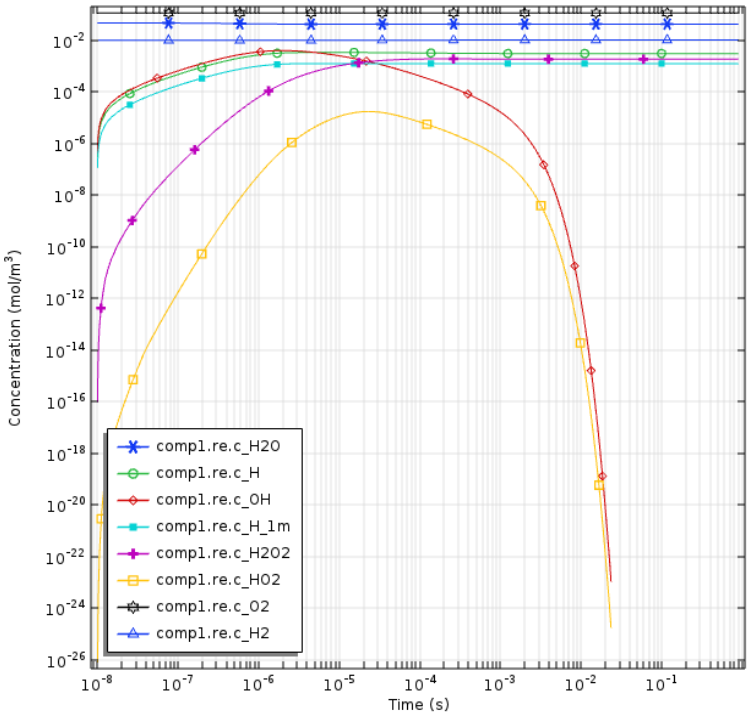

Figure 10. Concentration profiles of the outlet species versus the evolution time with dissociative attachment reaction (H^-).

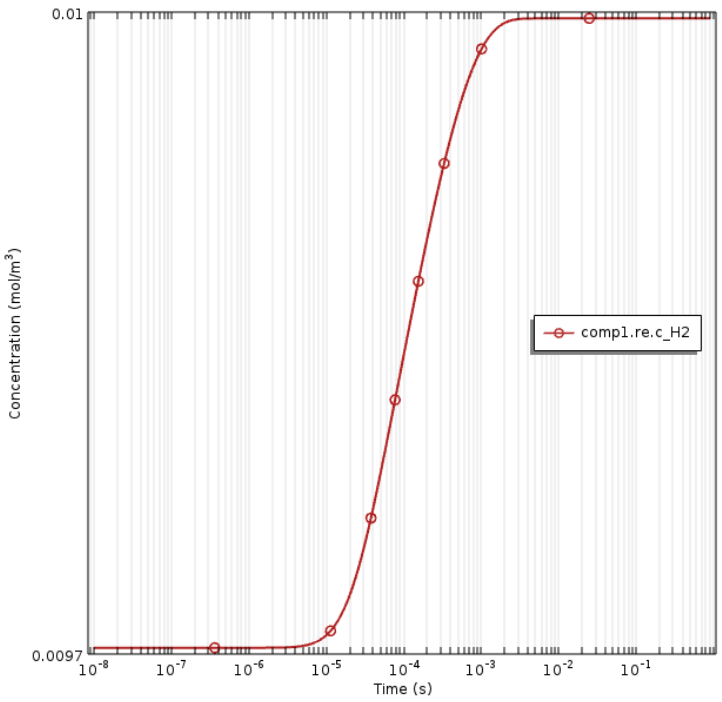

Figure 11. H_2 concentration profile with dissociative attachment reaction (H^-).

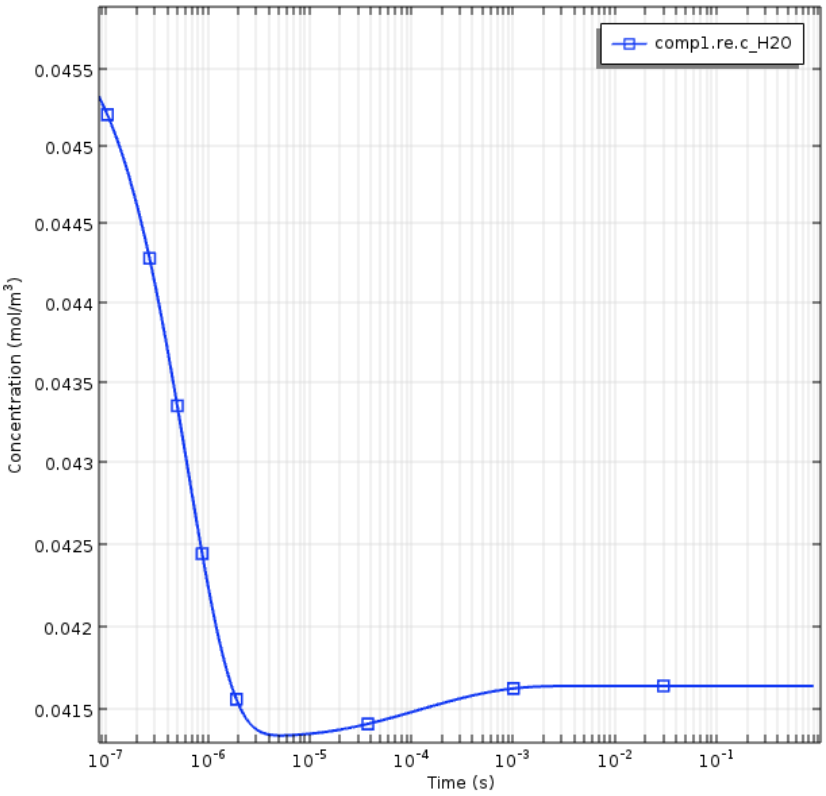

Figure 12. H_2O concentration profile with dissociative attachment reaction (H^-).

However, the concentration profile results of both simulation models are similar, but in the current simulation study, it was investigated the major products of these reaction mechanisms H_2 and O_2. Further, the simulation and experimental results were compared in the next section.

3.2.1. Comparison between theoretical and experimental results (Model II)

Figure (13) presents theoretical and experimental results of the effect of inlet water vapor temperature on the hydrogen concentration at plasma applied voltage of 12 kV. Compared with the simulation analysis without the dissociative attachment reaction, it was found that the hydrogen concentrations values dropped in a range of 50–62% by applying simulation analysis with dissociative attachment reaction. In addition, it was observed that the simulation results of hydrogen concentrations are nearly same as the experimental data due to add and start the water vapor breakdown with the dissociative attachment reaction. The hydrogen concentration results at different water vapor input temperatures and plasma applied voltage of 14 kV is shown in Figure (14). The results of the simulation and experimental results seem to be same, however, the concentration trend was not similar in both plasma applied voltage for the simulation model with dissociative attachment reaction.

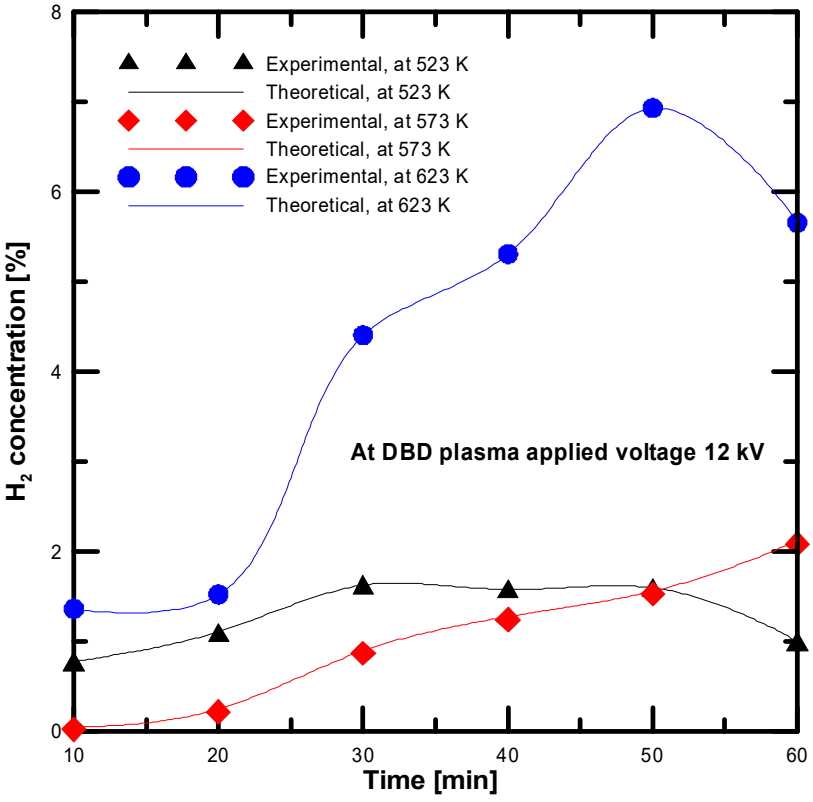

Figure 13. *Comparison* between experimental and theoretical steam decomposition concentrations data at plasma voltage 12 kV.

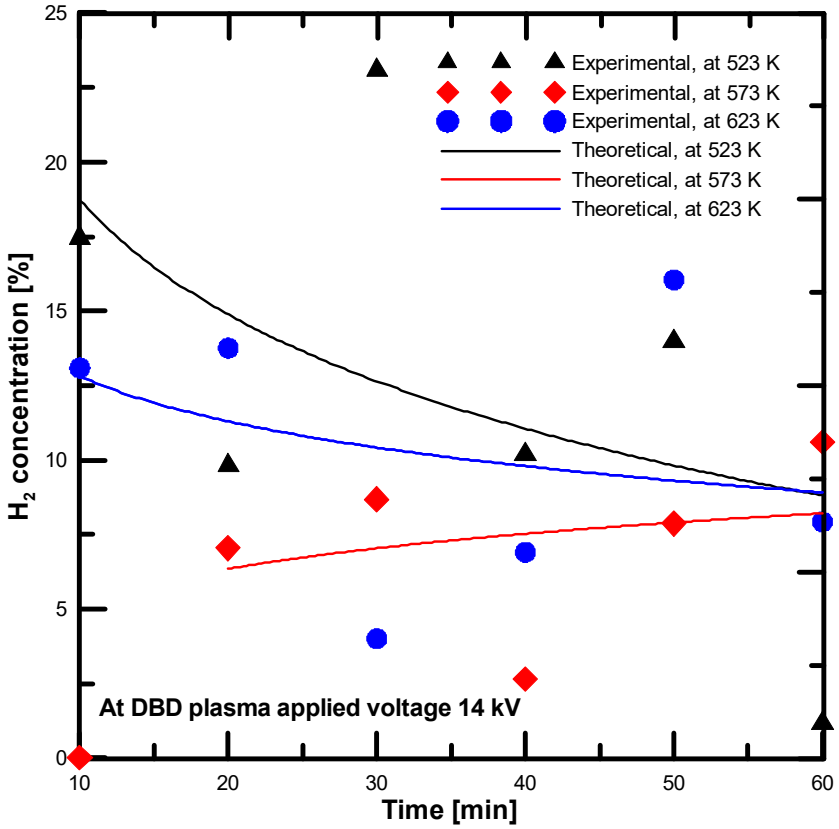

Figure 14. Comparison between experimental and theoretical steam decomposition concentrations data at plasma voltage 14 kV.

Furthermore, it was found that the hydrogen concentrations of simulation model with dissociative attachment reaction at plasma voltage of 14 kV decreased from the simulation results obtained from simulation model without (H^-) radicals in a range of 10–16%. The simulation results of hydrogen concentration obtained at plasma voltage 14 kV are not linearly changed with the water vapor input temperatures because of the effect of plasma high voltage and high electron mobility of decomposed gas, while at plasma voltage 12 kV, the maximum obtained results of H_2 concentration at the highest input water vapor temperature. It is possibly changed due to sample collections during the experiment, some of hydrogen gas was not completely separated in the ice trap and some of separated hydrogen was remained inside the ice trap. To clarify the hydrogen concentration at different plasma voltage and at the same water vapor input temperature, Figure (15a, b, c) shows the effect of plasma voltage on the hydrogen concentration of experimental and simulation results with dissociative attachment reaction versus the reaction revolution time. It was found that the simulation results of hydrogen concentration at plasma voltage 14 kV was higher than that obtained from 12 kV at the same input water vapor temperature. The simulation model with the dissociative attachment reaction (H^-) showed a good agreement with the water vapor experimental results, it was found that the dissociative attachment reaction to be an important step in water vapor decomposition using DBD plasma. Furthermore, when the simulation was carried out with the dissociative attachment reaction mechanism (H^-), the hydrogen concentration dropped to be nearly same as the experimental results. Also, it was observed that the concentration of water molecules did not reach to zero, by

means that some of the water vapor molecules are condensed inside the ice trap and did not convert into H_2 and O_2 gas.

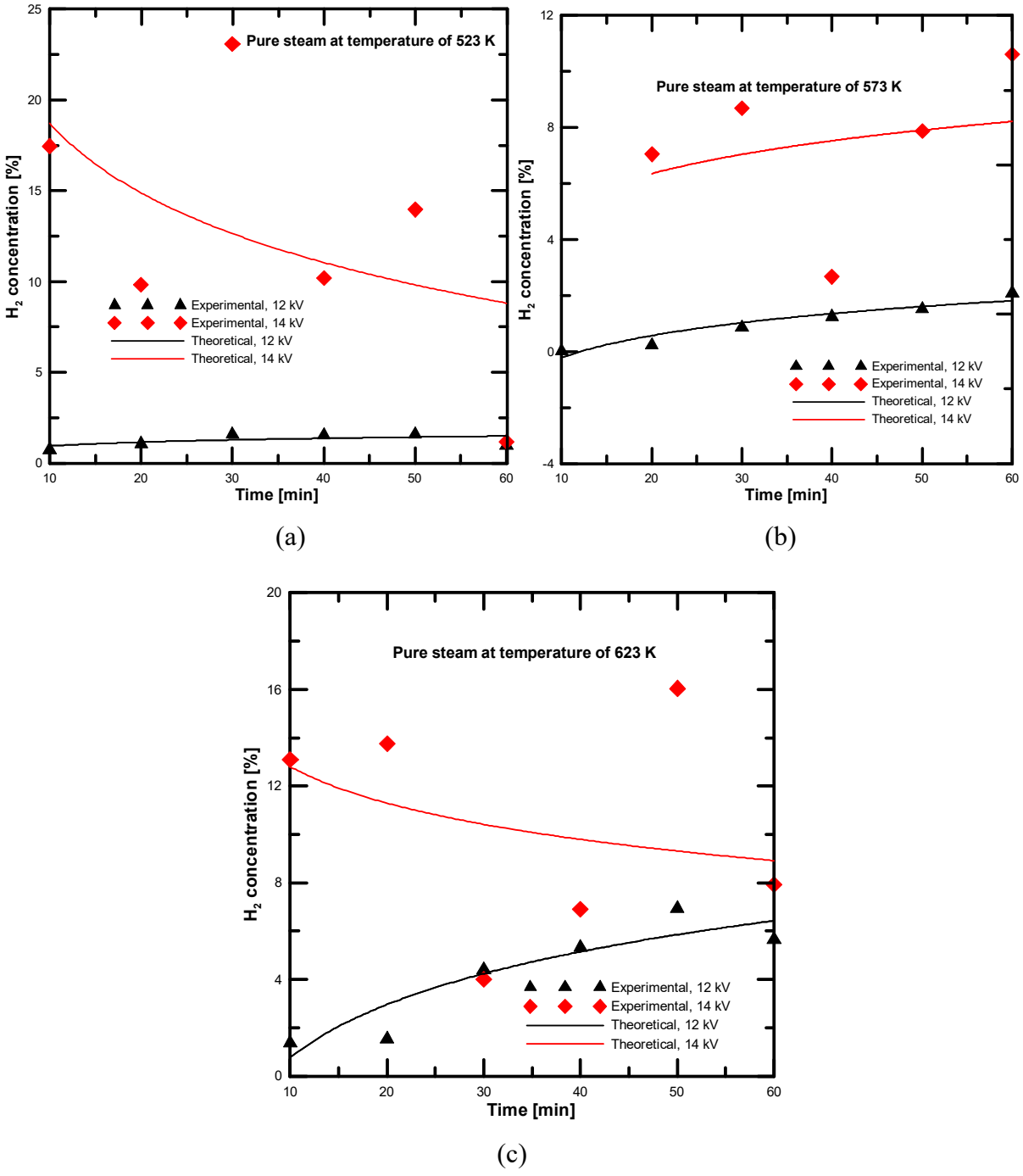

Figure 15. Comparison between experimental and theoretical steam decomposition concentrations at steam temperatures: a) 523 K, b) 573 K, c) 623 K.

3.3. Comparison between both simulation models reaction mechanism and experimental results

The conversion rate of both simulation models have been evaluated and compared between the water vapor decomposition using DBD plasma experimental results. The conversion rate can be determined according to the following expression: *conversion rate [%] = (F_{H2} [mole/min]/ F_{inH2O}*

[mole/min]) × 100. Where F_{H2} is the produced hydrogen gas and F_{inH2O} is the water vapour inlet flow rate. The water vapor was decomposed into their elements hydrogen and oxygen gas using DBD plasma. Figure (16) shows the conversion rate change of the hydrogen production from water vapor at different plasma voltage and at water vapor input temperature 523 K. The conversion rate of the simulation model with the dissociative attachment reaction showed good agreement with the conversion rate of the experimental results compared with the results of the simulation model without dissociative attachment reaction. The comparison between conversion rates of water vapor at input temperature of 573 K is presented in Figure (17). The conversion rate of the simulation models result showed more hydrogen production concentration values than that obtained from the experimental concentration values. In both simulation models, it was found that the dissociative attachment reaction has an important effect as a first step of the water vapor dissociation process using plasma. Furthermore, it was observed that the conversion rate of input water vapor temperature 573 K was lower than the conversion rate of input water vapor temperatures of 523 and 623 K.

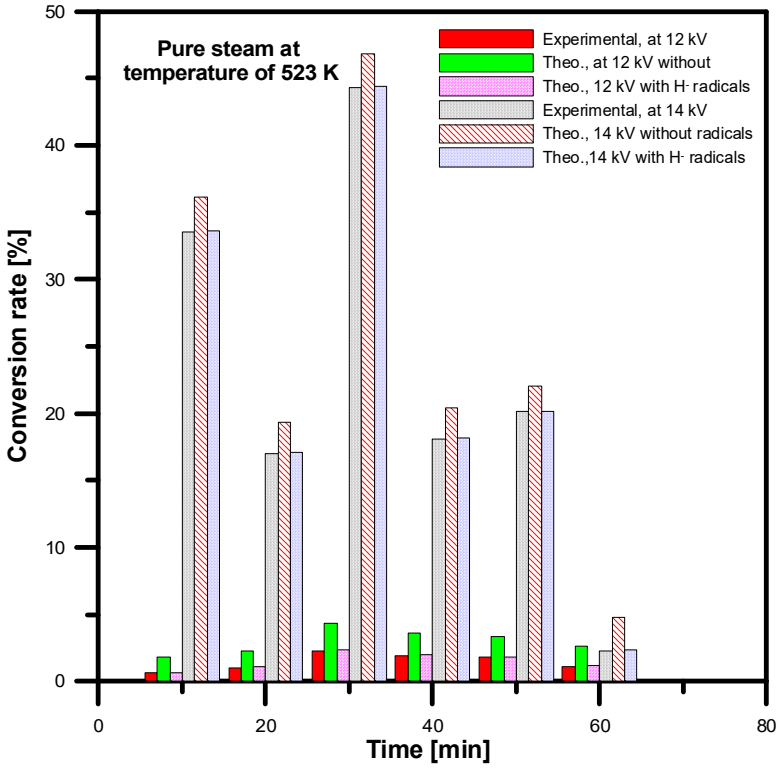

Figure 16. Conversion rate *comparison* of both reaction mechanisms at temperature of 523 K and different plasma voltage.

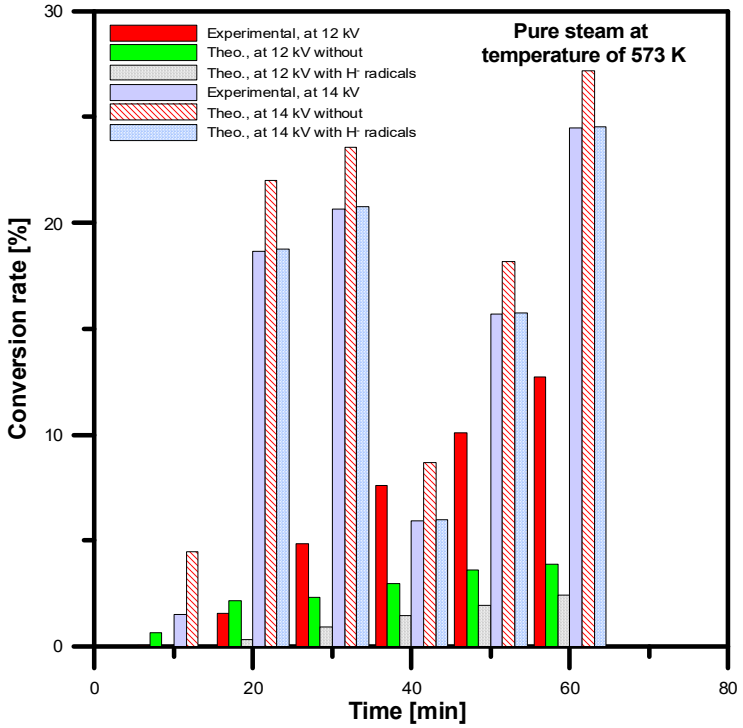

Figure 17. Conversion rate *comparison* of both reaction mechanisms at temperature of 573 K and different plasma voltage.

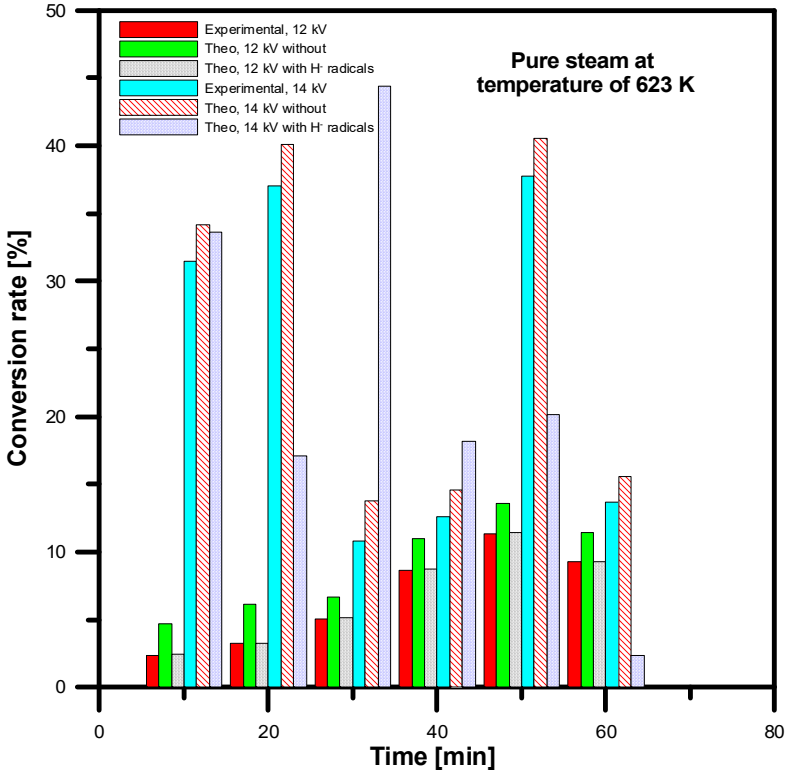

Figure 18. Conversion rate *comparison* of both reaction mechanisms at temperature of 623 K and different plasma voltage.

In addition, the conversion rate of input water vapor at temperature of 623 K is shown in Figure (18). The conversion rate results of the simulation model with dissociative attachment reaction seemed to be same in all water vapor input gas temperatures. Furthermore, it was found that the dissociation attachment reaction dominate the water vapor dissociation, in addition the hydrogen concentrations were dropped in both plasma applied voltages to be appeared same as the experimental results.

4. Conclusions

The simulation results showed that the dissociative attachment reaction and the dissociative reaction of electrons have an important effect on the water vapour breakdown processes. The simulation analysis showed that the hydrogen concentrations obtained from the simulation model with the dissociative attachment reaction were lower than those obtained from the simulation model deselecting the dissociative attachment reaction. The hydrogen concentration results of both models were compared with the experimental results. It was found that the hydrogen concentration results of the simulation model selecting the dissociative attachment reaction were nearly same as that obtained from the experimental results. It was observed that the concentration results dropped by the addition of H^- radical into the simulation model with the dissociative attachment reaction when used as a primary reaction of electron water vapour plasmolysis. Furthermore, it was concluded that the dissociative attachment reaction included H^- radical controlled the hydrogen production from the detachment electron. The conversion rates were determined for the simulation models and the experimental results. The conversion rate results showed that the simulation model with the dissociative attachment reaction has introduced more acceptable data to the experimental results of the water vapour plasmolysis dissociation reactions pathway.

Acknowledgments

The author would like to thank *Prof. Shinji Kambara* and Gifu University for their continuous support to this project.

Conflict of interest

The authors declare that they have no conflict of interest that could have appeared to influence the work reported in this paper.

References

1. Gupta NM (2016) Factors affecting the efficiency of a water splitting photo catalyst: A perspective. *Renewable Sustainable Energy Rev* 71: 585–601.
2. Dubey PK, Tripathi P, Tiwari RS, et al. (2014) Synthesis of reduced graphene oxide-TiO_2 nanoparticle composite systems and its application in hydrogen production. *Int J Hydrogen Energy* 39: 16282–16292.
3. Dincer I (2002) Technical, environmental and exergetic aspects of hydrogen energy systems. *Int J Hydrogen Energy* 27: 265–285.
4. Dincer I (2012) Green methods for hydrogen production. *Int J Hydrogen Energy* 37: 1954–71.

5. Barreto L, Makihira A, Riahi K (2003) The hydrogen economy in the 21st century: A sustainable development scenario. *Int J Hydrogen Energy* 28: 267–284.
6. Midilli A, Dincer I (2007) Key strategies of hydrogen energy systems for sustainability. *Int J Hydrogen Energy* 32: 511–524.
7. Abe JO, Popoola IPA, Ajenifuja E, et al. (2019) Hydrogen energy, economy and storage: Review and recommendation. *Int J Hydrogen Energy* 44: 15072–86.
8. Hoffman P (2019) *The Forever Fuel, The Story of Hydrogen*, 1st edition, Taylor & Francis group, eBook.
9. Holladay DJ, Hu J, King LD, et al. (2009) An overview of hydrogen production technologies. *Catal Today* 139: 244–260.
10. El-Shafie M, Kambara S, Hayakawa Y (2019) Hydrogen production technologies overview. *J Power Energy Eng* 7: 107–154.
11. Simpson AP, Lutz AE (2007) Exergy analysis of hydrogen production via steam methane reforming. *Int J Hydrogen Energy* 32: 4811–20.
12. Stefanidis GD, Vlachos DG (2010) Intensification of steam reforming of natural gas: choosing combustible fuel and reforming catalyst. *Chem Eng Sci* 65: 398–404.
13. Šingliar M (2007) Solar energy using for hydrogen production. *Pet Coal* 49: 40–47.
14. Guoxin H, Hao H, Yanhong L (2009) Hydrogen-rich gas production from pyrolysis of biomass in an auto generated steam atmosphere. *Energy Fuels* 23: 1748–53.
15. Bockris JOM, Dandapani B, Cocke D, et al. (1985) On the splitting of water. *Int J Hydrogen Energy* 10: 179–201.
16. El-Shafie M, Kambara S, Hayakawa Y, et al. (2019) Preliminary results of hydrogen production fromwater vapor decomposition using DBD plasma in a PMCR reactor. *Int J Hydrogen Energy* 44: 20239–48.
17. Givotov V, Fridman A, Krotov M, et al. (1981) Plasmochemical methods of hydrogen production. *Int J Hydrogen Energy* 6: 441–9.
18. Fridman AA (2008) Plasma chemistry. Cambridge University Press.
19. Maehara T, Toyota H, Kuramoto M, et al. (2006) Radio frequency plasma in water. *Jpn J Appl Phys* 45: 8864–8.
20. Nguyen SVT, Foster JE, Gallimore AD (2009) Operating a radiofrequency plasma source on water vapor. *Rev Sci Instrum* 80:083503.
21. Burlica R, Shih KY, Locke B (2010) Formation of H_2 and H_2O_2 in a water-spray gliding arc non thermal plasma reactor. *Ind Eng Chem Res*.
22. Mutaf-Yardimci O, Saveliev A, Fridman A, et al. (1998) Employing plasma as catalyst in hydrogen production. *Int J Hydrogen Energy* 23: 1109–11.
23. Xi Zhen L, Liu CJ, Eliasson B (2003) Hydrogen production from methanol using corona discharges. *Chin Chem Lett* 14: 631–3.
24. Sarmiento B, Brey JJ, Viera IG, et al. (2007) Hydrogen production by reforming of hydrocarbons and alcohols in a dielectric barrier discharge. *J Power Sources* 169: 140–3.
25. Rico VJ, Cotrino J, Gallardo V, et al. (2009) Hybrid catalytic-DBD plasma reactor for the production of hydrogen and preferential CO-oxidation (CO-PROX) at reduced temperatures. *Chem Commun* 41: 6192–4.
26. Wang W, Zhu C, Cao Y (2010) DFT study on pathways of steam reforming of ethanol under cold plasma conditions for hydrogen generation. *Int J Hydrogen Energy* 35: 1951–6.

27. Yan Z, Chen L, Wang H (2008) Hydrogen generation by glow discharge plasma electrolysis of ethanol solutions. *J Phys D: Appl Phys* 41: 155205.
28. Rehman F, Lozano-Parada JH, Zimmerman WB (2012) A kinetic model for H_2 production by plasmolysis of water vapours at atmospheric pressure in a dielectric barrier discharge micro channel reactor. *Int J Hydrogen Energy* 37: 17678–90.
29. Jasinski M, Dors M, Mizeraczyk J (2008) Production of hydrogen via methane reforming using atmospheric pressure microwave plasma. *J Power Sour* 181: 41–5.
30. Sobacchi M, Saveliev A, Fridman A, et al. (2002) Experimental assessment of a combined plasma/catalytic system for hydrogen production via partial oxidation of hydrocarbon fuels. *Int J Hydrogen Energy* 27: 635–42.
31. Avtaeva S, General A, Kel'man V (2010) Kinetic model for low density non-stationary gas discharge in water vapour. *J Phys D: Appl Phys* 43: 315201.
32. Dolan T (1993) Electron and ion collisions with water vapour. *J Phys D: Appl Phys* 26: 4.
33. Medodovic S, Locke B (2009) Primary chemical reactions in pulsed electrical discharge channels in water. *J Phys D: Appl Phys* 42: 049801.
34. Lukes P, Clupek M, Babicky V, et al. (2008) Role of solution conductivity in the electron impact dissociation of H_2O induced by plasma processes in the pulsed corona discharge in water. *HAKONE XI, 11th international symposium on high pressure, low temperature plasma chemistry*, contributed papers, Ole´ron Island.
35. Shirafuji T, Morita T, Sakai O, et al. (2009) Enhancement of OH production rate in plasma on water by mixing Ar. *Proceedings of the international symposium on plasma on plasma chemistry*, Bochum, Germany.
36. Locke B, Sato M, Sunka P, et al. (2006) Electrohydraulic discharge and nonthermal plasma for water treatment. *Ind Eng Chem Res* 45: 882–905.
37. Zimmerman WBJ (2006) Multiphysics modeling with finite element methods, series on stability, vibration and control of systems, series A. *London: World Scientific Publishing Company*.
38. Lozano-Parada JH, Zimmerman WB (2010) The role of kinetics in the design of plasma microreactors. *Chem Eng Sci* 65: 4925–30.
39. Zhang Y, Wen XH, Yang WH (2007) Excitation temperatures of atmospheric argon in dielectric barrier discharges. *Plasma Sources Sci Technol* 16: 441.
40. Nehra V, Kumar A, Dwivedi H (2008) Atmospheric non-thermal plasma sources. *Int J Eng* 2: 53.
41. Abdul-Majeed WS, Parada JHL, Zimmerman WB (2011) Optimization of a miniaturized DBD plasma chip for mercury detection in water samples. *Anal Bioanal Chem* 401: 2713–22.
42. Zito JC, Arnold DP, Durscher RJ, et al. (2010) Investigation of impedance characteristics and power delivery for dielectric barrier discharge plasma actuators. In: *48th AIAA Aerospace Sciences Meeting.*
43. Kostov K, Honda R, Alves L, et al. (2009) Characteristics of dielectric barrier discharge reactor for material treatment. *Braz J Phys* 39: 322–5.
44. Rehman F, Liu Y, Zimmerman WBJ (2016) The role of chemical kinetics in using O_3 generation as proxy for hydrogen production from water vapour plasmolysis. *Int J Hydrogen Energy* 41: 6180–92.
45. Shih KY, Locke BR (2010) Optical and electrical diagnostics of the effects of conductivity on liquid phase electrical discharge. *IEEE Trans Plasma Sci* 99: 1–10.

46. El-Shafie M, Kambara S, Hayakawa Y (2020) One-dimensional simulation of hydrogen production kinetic models by water vapor plasmolysis in a DBD plate reactor. *J Theor Appl Phys* 14: 181–194.